INTERNATIONAL JOURNAL FOR NUMERICAL METHODS IN FLUIDS, VOL. 4, 171–183 (1984)

SIMULATION OF POLYMERIC FLOWS IN THE INJECTION MOULDING PROCESS*

SHAN-FU SHEN

Sibley School of Mechanical and Aerospace Engineering, Cornell University, Ithaca, New York 14853, U.S.A.

SUMMARY

Recent progress in the simulation of polymeric flows of two key problems in the injection moulding process, carried out by a team at Cornell University, is briefly described. For the filling of cooled thin cavities, the fluid is characterized by a power-law viscosity with exponential temperature dependence, and interaction between the transient thermal boundary-layer and the core flow in a domain with moving boundary is essential. The earlier procedure of Hieber and Shen is modified in two aspects: a boundary-integral formulation replaces the finite-element treatment of the pressure, and an 'energy integral' approach is used for the transient temperature. The second problem is the steady visco-elastic flow in the juncture region where sudden changes of the geometry and large strain rates occur. The constitutive equation is postulated according to the Leonov model. The main features in the numerical implementation are: integration along a streamline to determine the elastic deformation tensors for a given velocity field, and finite-element treatment (in time-dependent form) of the pressure and fields for given stresses. In an example where the contraction ratio is 7:1, results for nominal Deborah number exceeding 100 show no numerical instability. (However, for this problem, the true Weissenberg number, i.e. the ratio of local first-normal-stress difference to shear stress turns out to be generally $O(10)$.) The predictions also correlate very well with experimental birefringence measurements.

KEY WORDS Polymer Flows Non-Newtonian Moving Boundary

INTRODUCTION

Injection moulding is a widely used industrial process, which manufactures plastic parts by forcing molten polymer into a cavity followed by solidification. A team at Cornell, under NSF sponsorship and with industrial co-operation, has engaged in research on various problems of the injection moulding process since 1973. As may be obvious, flow analysis must be one of primary interest, and the finite-element method has been a most important tool. However, for polymeric fluids the shear viscosity is not only rate-dependent but highly sensitive to small changes of temperature. Interaction of the velocity and temperature fields becomes a central feature. In other than shear-dominated flows, to describe the stresses properly requires a phenomenologically realistic general constitutive equation. Moreover, practical operations involve very high rates of deformation, say $O(100)\,s^{-1}$. For meaningful practical predictions, these are formidable challenges.

The following describes the recent progress on two problems which have been attacked by the Cornell team via the finite-element technique: the filling of a thin cavity of arbitrary plan form and the visco-elastic flow near a juncture. Neither is a straightforward boundary-value

* This invited paper is an extended, and refereed version of one presented at the Fourth International Symposium on Finite Elements in Flow Problems held in Tokyo, Japan, 26–29 July 1982.

0271–2091/84/020171–13$01.30

Received 5 January 1983
Revised 4 May 1983

problem. The cavity-filling features a moving free-surface and the interaction with a transient thermal layer. Our earlier work was summarized by Hieber and Shen.[1] As an alternative a boundary-integral formulation has been developed by Kwon.[2] It is at least competitive, and may be worthy of further exploration. In the juncture problem, the memory effects have caused difficulties known to all previous investigators of the entrance effects, which occur at the sudden contraction of a circular pipe. As the Deborah number De reaches $O(1)$, $De \equiv \dot{\gamma}_a \theta$, $\dot{\gamma}_a$ being the apparent shear rate and θ the reference relaxation time, numerical instability has been a serious problem. We encountered similar syndromes in a FEM program using the linear Maxwell model as the constitutive equation, reported by Morjaria;[3] for an important recent attempt to improve such calculations, see References 4 and 5. In real problems, to describe the elastic effects properly demands the use of a more accurate constitutive equation. The model lately proposed by Leonov[6] seems to cover our range of interest (see also Reference 7, where an essentially similar model was independently derived). A series of investigations[8–10] now convince us that it should serve as a prime candidate for the simulation of more general visco-elastic flows. Further, the Leonov model has the practical advantage of more straightforward implementation when compared with the memory integral formulation used in Reference 4. The finite-element treatment described below is due to Upadhyay.[11] In a two-dimensional test case, his results show good agreement with experiment while reaching a nominal De of $O(100)$ without numerical difficulty. A better measure of elastic effects is the Weissenberg number We (the first normal-stress difference divided by the shear stress), which of course varies from point to point but generally is found to be $O(10)$ in the calculated example.

FILLING OF A THIN CAVITY

We consider a thin cavity within a solid mould of arbitrary plan form, as shown in Figure 1. In Cartesian co-ordinates the plan form is bounded by the outer contour C_o in the x, y plane; the gap thickness $2b(x, y)$ in the z-direction is much smaller than the length scale defining C_o. The fluid enters the cavity across the entry contour C_e, and as time t progresses, occupies a region extending to the moving front $C_m(t)$. There may be also impermeable contours C_i within C_o. In injection moulding the inertial terms are found to be negligible, and the thin-gap configuration enables the equations to be simplified by the Hele–Shaw approxima-

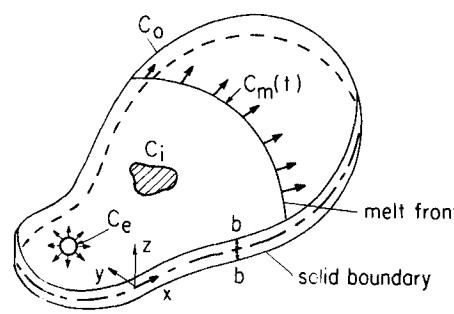

Figure 1. Sketch of a thin cavity and the co-ordinate system

tion:

$$0 = \frac{\partial}{\partial z}\left(\eta \frac{\partial u}{\partial z}\right) - \frac{\partial p}{\partial x} \tag{1}$$

$$0 = \frac{\partial}{\partial z}\left(\eta \frac{\partial v}{\partial z}\right) - \frac{\partial p}{\partial y} \tag{2}$$

$$\frac{\partial u}{\partial x} + \frac{\partial v}{\partial y} + \frac{\partial w}{\partial z} = 0 \tag{3}$$

where (u, v, w) are the velocity components in the x-, y- and z-directions, respectively, η is the apparent shear viscosity and p is the pressure (constant in the z-direction). Following Williams and Lord,[12] the viscosity of the polymeric fluid is characterized by the inelastic model $\eta = \eta(\dot{\gamma}, T)$, where

$$\dot{\gamma} = \sqrt{\left[\left(\frac{\partial u}{\partial z}\right)^2 + \left(\frac{\partial v}{\partial z}\right)^2\right]}$$

and T is the temperature. The temperature field is described by the energy equation, simplified again through the thin-gap approximation,

$$\rho C_p\left(\frac{\partial T}{\partial t} + u\frac{\partial T}{\partial x} + v\frac{\partial T}{\partial y} + w\frac{\partial T}{\partial z}\right) = \eta\dot{\gamma}^2 + k\frac{\partial^2 T}{\partial z^2} \tag{4}$$

where ρ is the fluid density, C_p the specific heat and k the thermal conductivity (assumed constant). All the left-hand side terms are retained because for polymeric fluids the Péclét number is large.

With a given $\eta(x, y, z, t)$ and no slip at the wall, equations (1) and (2) are easily integrated. In terms of the gapwise averaged velocity components $(\bar{u}, \bar{v})$, the result is, for usual applications where η is symmetric in z,

$$\bar{u} \equiv \frac{1}{2b}\int_{-b}^{b} u\,dz = -\frac{S}{2b}\frac{\partial p}{\partial x}, \qquad \bar{v} \equiv \frac{1}{2b}\int_{-b}^{b} v\,dz = -\frac{S}{2b}\frac{\partial p}{\partial y} \tag{5}$$

with

$$S = \int_{-b}^{b} (z^2/\eta)\,dz \tag{6}$$

Integration of equation (3) also across the gap finally leads to, with equation (5),

$$\nabla \cdot S\nabla p = 0 \tag{7}$$

∇ being the two-dimensional Laplace operator in the x, y-plane.

If the temperature is known, equation (7) is quasi-linear in p and resembles the equation governing the velocity potential in subsonic compressible flows. At each instant we have a boundary value problem with normal gradients (normal velocity) specified along C_e, C_i and C_o, and a back pressure specified along C_m. But S depends on $\bar{u}$, $\bar{v}$ and also the temperature, which should be determined from equation (4) simultaneously. In contrast to $\bar{u}$ and $\bar{v}$ which contain the time t as a parameter only, the temperature is a true transient three-dimensional field. Its variation at entry and along the wall must be prescribed. As the fluid spreads in the cavity, a thermal boundary layer grows on the mould wall between the entry and the moving front. Its temporal and spatial variations change the course of the subsequent flow.

In Reference 1 the solution of the above system was carried out by allowing the temperature field to lag one time step Δt behind the velocity field. The known temperature field determined the pressure and velocity at t. The velocity field was then used both to advance the front C_m and determine the new temperature field for the next time step. The procedure was repeated until the fluid filled the cavity. In essence, equation (7) was solved iteratively at each time step by a finite-element method, with new elements added as the front moved forward. The temperature field, on the other hand, required a combined finite element (in the x, y plane) and finite difference (in the z- and t-directions) treatment. The most time consuming part turned out to be the extremely slow convergence of the iterative determination of the coefficient S. A more efficient solver for equation (7) is therefore desirable.

Boundary-integral formulation of equation (8) *for power law fluid*

As in Reference 1 the viscosity law is specified to be

$$\eta = m_0 \dot{\gamma}^{n-1} \exp(-T_a/T) \tag{8}$$

where n is the 'power law index', $n<1$ (shear thinning), and m_0 and T_a are material constants. From equation (8) it follows that

$$S = |\nabla p|^{1-n/n} m_0^{1/n} \bar{\mathscr{P}} \tag{9}$$

where

$$\bar{\mathscr{P}} \equiv \int_0^b z^{1+1/n} \exp[-T_a/nT]\, dz \tag{10}$$

In this case the temperature effects are felt only through $\bar{\mathscr{P}}$.

Let equation (7) be rewritten as

$$\nabla^2 p = -\frac{1}{S} \nabla S \cdot \nabla p = f \text{ (say)} \tag{11}$$

For given f, equation (11) is a Poisson equation and the solution in the region Ω bounded by contour C (Figure 2) satisfies

$$\beta p(x, y) = \int_C \left[p \frac{\partial}{\partial n} (\ln r) - (\ln r) \frac{\partial p}{\partial n} \right] ds + \int_\Omega f(\ln r)\, d\Omega \tag{12}$$

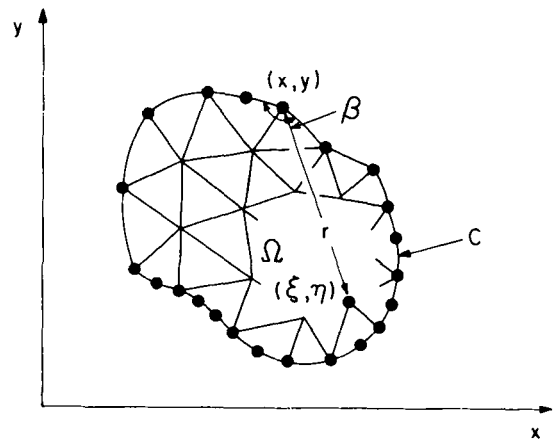

Figure 2. Symbols used in the boundary-integral formulation

In equation (12), β is the interior angle for points on C, but equals 2π for interior points, $r=[(x-\xi)^2+(y-\eta)^2]^{1/2}$, (ξ, η) being the co-ordinates of the variable points over which the integral is performed; ds is a length element along C, n is the outward normal direction, and $d\Omega$ the area element in Ω. Note that for the assumed power law model,

$$f=-(f_1+f_2)$$
$$f_1=\frac{1-n}{n}(p_x^2p_{xx}+2p_xp_yp_{xy}+p_y^2p_{yy})/(p_x^2+p_y^2) \tag{13}$$
$$f_2=(p_x\bar{\mathscr{P}}_x+p_y\bar{\mathscr{P}}_y)/\bar{\mathscr{P}}$$

where the subscripts indicate partial derivatives. Thus, if $b=\text{const.}$, f_1 gives the shear-thinning effects and f_2 gives the non-isothermal effects.

Equation (12) is of course a classical result in potential theory. Systematic treatments along the lines of the finite-element method are of more recent origin.[13,14] At any rate, with f known and either p or $\partial p/\partial n$ prescribed at each point along C, equation (12) can be discretized into boundary elements to determine the missing data of p or $\partial p/\partial n$ along C. The unknown values of p in the interior points, if desired, are obtained by quadrature, again using equation (12) but $\beta=2\pi$. The derivatives of p at any point can be given by expressions similar to equation (12). Unlike the finite element method, the derivatives need not suffer from the inaccuracy due to local interpolation.

The boundary-integral treatment of cavity-filling has been carried out by Kwon.[2] The general procedure follows that of Reference 1. The flow at the end of the first time step is confined in a small region next to the gate, and may be approximated by assuming isothermal conditions. At later times, the temperature field is taken as given and equation (12) is solved with the domain integral treated as known. Since the latter depends on the pressure field, iteration is necessary and under-relaxation is found to lead to better convergence. After the convergent p, p_x, p_y are obtained, they can be easily adjusted by a multiplicative factor to satisfy the constraint of specified volume flow rate as described in Reference 1. To evaluate the domain integral, a number of triangular internal elements are introduced, shown in Figure 2. After each iteration the nodal values of f are evaluated and a linear interpolation in each element is assumed. The contribution by each element to the domain integral is then calculated by Gaussian quadrature. The converged solution provides, among other things, $\partial p/\partial n$ and hence the normal velocity along the moving front $C_m(t)$, causing its advancement to the new position during the next time step.

It remains to update the temperature field before the pressure distribution in the new domain can be calculated. The analysis of equation (4) in Reference 1 was to treat it as a transient problem in (z, t) for the temperature values at the nodal points of the finite element mesh, with the flow as determined from the previous time step. The temperature within each element was obtained by interpolation, and the transient problem was solved by a finite-difference procedure. Worth mentioning is that aside from the usual boundary conditions, the large Pe and thin gap approximations require that the temperature at the moving front should be assigned as that of the melt upon entry at the gate. In Reference 1 also is described a simple scheme for upwinding that suppresses numerical instability. For the boundary-integral program, however, the finite-element mesh in the (x, y)-plane is only of secondary importance, and an alternative approach seems desirable.

Thus, proceeding as in the classical integral method for boundary layers, Kwon developed an 'integral energy method', which was earlier studied by Wang[15] in a simplified context of the present problem. Basically, equation (4) is integrated across the gap. With equations (3),

(5), (6), (8), (9), (10) and the boundary conditions, the results may be reduced to the form

$$\rho C_p\left(\frac{\partial \bar{T}}{\partial t}+\bar{u}\frac{\partial T^*}{\partial x}+\bar{v}\frac{\partial T^*}{\partial y}\right)=\frac{1}{b}k\frac{\partial T}{\partial z}\bigg|_{z=b}+\frac{1}{b}\frac{\Lambda^{n+1/n}}{m_0^{1/n}}\bar{\mathscr{P}} \tag{14}$$

where

$$\bar{T}=\int_0^b T\,\mathrm{d}z/b$$

the gap-averaged temperature

$$T^*=\int_0^b \sqrt{(u^2+v^2)}T\,\mathrm{d}z\Big/\int_0^b \sqrt{(u^2+v^2)}\,\mathrm{d}z$$

the usual 'bulk temperature' defined with respect to the local resultant velocity.

Equation (14) is now a transient problem in the (x, y)-plane. Note that the convective action is *only* along the gap-averaged velocity direction!

If the temperature distribution is adequately represented by a family of curves with one parameter, say a thermal 'boundary thickness' h, all dependence on T can be rewritten in terms of h and equation (14) eventually becomes of the form

$$A(h,\ldots)\,\partial h/\partial t+\bar{u}\,\partial h/\partial x+\bar{v}\,\partial h/\partial y=B(h,\ldots) \tag{15}$$

where $A(h,\ldots)$ and $B(h,\ldots)$ also involve the velocity field solution. In principle, the evolution of temperature can be traced by following the trajectories defined by the gap-averaged velocity, with the specified melt temperature prescribed both at the entry and at the front. Along each of the trajectories the problem is quite analogous to the degenerate one studied by Wang[15] which has only one spatial dimension.

For specific calculations, the simplest representation of a linear profile in the thermal layer of thickness h and constant (equal to the melt temperature) in the core region outside the thermal layer has been explored in Reference 15 and also adopted in Reference 2 for the more general case. In fact, Kwon decided to mimic Reference 1 by again introducing a triangular finite-element mesh and using the nodal temperature as the unknowns. The same procedures regarding interpolation averaging at a node, upwinding and the region adjacent to the front were retained.† The main difference from Reference 1 now lies in further reducing the transient problem in (z, t) to one in t only. For better accuracy, to go from $h(t)$ to $h(t+\Delta t)$ by an explicit difference scheme was achieved in two steps, the non-linear coefficients being calculated with $h(t+\frac{1}{2}\Delta t)$ obtained in the intermediate step. When compared with the more elaborate method of Reference 1, the predictions of fill pattern and pressure history by the integral method appear to be of the same order of accuracy in all cases so far studied, the gross nature of the linear profile in the thermal layer notwithstanding. Further details will be omitted here.

Example: an end-gated circular disk

The filling of a circular disk of diameter 4·44 cm and half-gap thickness 0·0794 cm, fed through a 'point gate' at one end, has been calculated by Kwon.[2] The material is polystyrene with the following properties: $n=0{\cdot}32$, $\rho=1{\cdot}05\ \mathrm{g/cm^3}$, $C_p=1{\cdot}84\times10^7\ \mathrm{erg/g\,K}$, $k=1{\cdot}26\times10^4\ \mathrm{erg/s\,cm\,K}$, $m_0=8{\cdot}01\ \mathrm{g/cm(s)^{1{\cdot}68}}$, $T_a=3635\ \mathrm{K}$. The flow conditions are: entry temperature $T_e=528\ \mathrm{K}$, wall temperature $T_w=241\ \mathrm{K}$, and flow rate $Q=5{\cdot}41\ \mathrm{cm^3/s}$.

† The upwinding scheme of Reference 1 was indeed very crude and should be further examined, as pointed out by a reviewer, but the convective contributions are typically small in the present problem except locally near the entrance. This was clearly demonstrated in Reference 15 without *ad hoc* upwinding. The assumed linear profile, for instance, probably also causes a significant error.

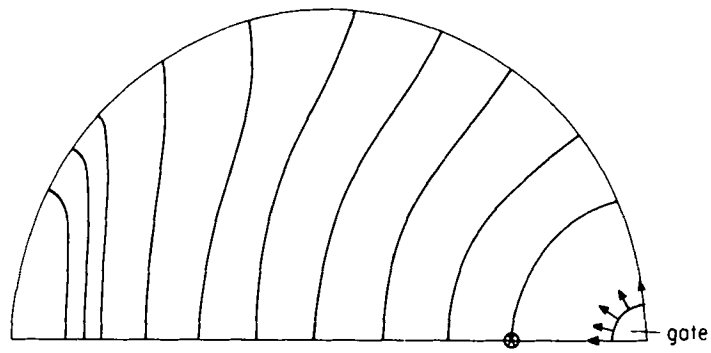

Figure 3. Non-isothermal fill-pattern of an end-gated circular disk; polystyrene as a power-law fluid, constant volume rate of flow

In Figure 3 is shown the front position at successive times. The pattern has been compared against that for a Newtonian isothermal fluid, in which case equation (12) reduces to the classical form for a Laplace equation without the domain integral, and is readily solved without iteration. The two patterns are extremely close to each other. This surprising result is not difficult to understand, at least from hindsight. For, given the same flow rate, the two patterns must be of equal area at the same instant. The contour C_m must be normal to the centreline as well as to the wall. With these constraints, unless the front is highly curvaceous it cannot greatly deviate from the Newtonian one. In other words, for simple cavities like the given example, the contour $C_m(t)$ is not a critical test of the method of solution. The pressure distribution required by the pattern is, of course, an entirely different matter.

Figure 4 shows the comparison of Kwon's prediction of the pressure history at one point against that computed from the FEM/FDM program of Reference 1. Although a slight systematic discrepancy is evident, both calculations actually used rather coarse meshes because of the tedious nature and expensive cost, and the relative accuracy is unclear. The comparison should only be considered as program verification. As for possible savings in computing time, a thorough study has yet to be made.

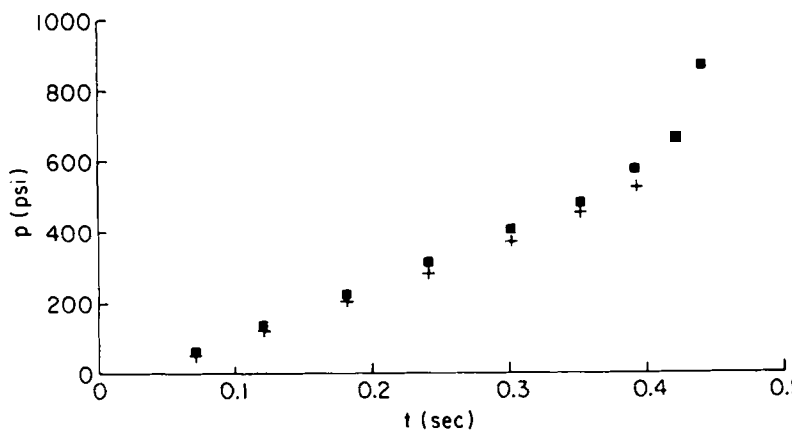

Figure 4. Pressure history at station marked × in Figure 3; ■ according to Reference 1, + by present BIM

VISCO-ELASTIC FLOW NEAR A JUNCTURE

The region where any sudden change of cross-section of an internal flow occurs may be called a juncture. In particular, the simple configurations in Figure 5, either two-dimensional or axi-symmetric, have long been of intense interest to rheologists because of their occurrence in typical rheometers. Unlike in the cavity-filling problem, the deformation in the juncture region is not dominated by shear only. A general creeping flow without the Hele–Shaw approximation must be analysed and the constitutive equation should be visco-elastic.

The governing equations are still those of equilibrium and continuity,

$$\nabla \cdot (-p\mathbf{I} + \boldsymbol{\tau}') = 0 \tag{16}$$

$$\nabla \cdot \mathbf{v} = 0 \tag{17}$$

where p is the pressure, $\mathbf{I}$ the unit tensor, $\boldsymbol{\tau}'$ the deviatoric part of the stress tensor, and $\mathbf{v}$ the velocity vector. A simple constitutive equation relating $\boldsymbol{\tau}'$ to the rate of deformation tensor $\boldsymbol{\varepsilon}$, twice the symmetrical part of $\nabla\mathbf{v}$, is the classical linear Maxwell model

$$\boldsymbol{\tau}' + \theta \frac{\delta}{\delta t}\boldsymbol{\tau}' = \eta\boldsymbol{\varepsilon} \tag{18}$$

$$\frac{\delta}{\delta t}\boldsymbol{\tau}' = \frac{\partial}{\partial t}\boldsymbol{\tau}' + \mathbf{v}\cdot\nabla\boldsymbol{\tau}' - (\nabla\mathbf{v})^T\cdot\boldsymbol{\tau}' - \boldsymbol{\tau}'\cdot\nabla\mathbf{v}, \tag{19}$$

$(\nabla\mathbf{v})^T$ being the transpose of $\nabla\mathbf{v}$. Even for steady flows, equations (18) and (19) show that a non-vanishing relaxation time causes the stress to be determined from a convective-type differential equation, exhibiting therby a 'memory effect'. For other popular models of the constitutive equation, see, e.g. Reference 16. The Deborah number *De* is a convenient parameter for the visco-elastic effect by comparing the relaxation time against the (inverse) shear rate, which represents the time constant of deformation. As mentioned above, our interest is for flows at large *De*, for which the Leonov model holds considerable promise, since it was designed especially with large elastic effects in mind.

Finite-element method for a Leonov fluid

Following Leonov,[6] contributions to the stress tensor $\boldsymbol{\tau}'$ due to the viscous and the elastic deformations are superposed, and further the elastic contribution is decomposed into a number of modes, for each of which, e.g. the kth mode, an elastic deformation tensor $\mathbf{C}^{(k)}$ is introduced. Without digression into its lengthy derivation, the constitutive equation with N

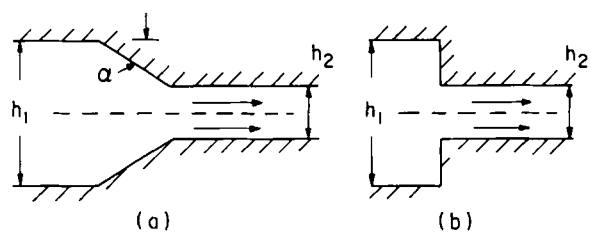

Figure 5. Typical juncture geometry: two-dimensional parallel channels with sudden or linear contraction

modes turns out to be of the form

$$\tau' = \eta_o s\varepsilon + \sum_{k=1}^{N} (\eta_k/\theta_k)\mathbf{C}^k \tag{20}$$

where η_o is the zero-shear-rate (Newtonian) viscosity, η_k and θ_k are respectively the shear viscosity and relaxation time of the kth mode, and $0<s<1$ is a rheological constant. The equation satisfied by $\mathbf{C}^{(k)}$ is uncoupled from other modes,

$$\frac{\delta}{\delta t}\mathbf{C}^{(k)} + \frac{1}{2\theta_k}(\mathbf{C}^{(k)} \cdot \mathbf{C}^{(k)} - \mathbf{I}) = 0 \tag{21}$$

the convective derivative $\delta/\delta t$ being as defined in equation (19). As the elastic effects tend to zero in a steady flow, equation (21) gives

$$\mathbf{C}^{(k)} \approx \mathbf{I} + \theta_k \boldsymbol{\varepsilon} \tag{22}$$

Hence, to reproduce the Newtonian behaviour at vanishing shear rates, equation (20) requires

$$\eta_0 = \sum_{k=1}^{N} \eta_k (1-s)^{-1} \tag{23}$$

Further, for self-consistency there is a constraint on $\mathbf{C}^{(k)}$, which for two-dimensional flows is simply

$$C_{11}^{(k)} C_{22}^{(k)} - (C_{12}^{(k)})^2 = 1 \tag{24}$$

where $C_{ij}^{(k)}$ denotes the ij component of $\mathbf{C}^{(k)}$. It turns out that all the material constants *can be determined from standard experiment*, e.g. the steady flow through a capillary rheometer or the dynamic response with oscillatory plates. As shown in References 8, 9 and 10, the Leonov model performs well in predicting the results of a host of different transient visco-elastic experiments on the basis of the constants chosen to fit standard characterization curves.

Given a two-dimensional juncture such as those in Figure 5, the equations to be solved are, to recapitulate, equations (16) and (17) together with (20), (21) and (24) for the Leonov model. Schematically, equations (16) and (17) define a creeping flow problem with the non-Newtonian stress field to be iterated until convergence. This being basically a boundary-value problem, the FEM formulation is straightforward. The system or equations (20), (21) and (24) defines how the stresses are evaluated from the velocity field via $\mathbf{C}^{(k)}$. If $\mathbf{v}$ is assumed known, equation (21) shows that the modes are uncoupled, and working with a multi-mode Leonov model does not greatly add complexity. Although tracking the distortion of fluid elements is not needed, the strongly convective nature of the operator in equation (21) should be handled with care. For steady flows, the FEM program should include upwinding. An earlier program made by Hieber (unpublished) to attack an entrance flow with a 2:1 contraction ratio was reasonably successful, but his upwinding scheme was rather crude.

The more recent FEM program of Upadhyay[11] for steady flows has the following main features: (i) integrating equation (21) for $\mathbf{C}^{(k)}$ along each streamline, in true Lagrandian sense; and (ii) recasting the iterations for $\mathbf{v}$ and p as a pseudo-unsteady process. Specifically, equation (21) is written as

$$|\mathbf{v}| \frac{\mathrm{d}\mathbf{C}^{(k)}}{\mathrm{d}\xi} = (\nabla \mathbf{v})^T \cdot \mathbf{C}^{(k)} + \mathbf{C}^{(k)} \cdot (\nabla \mathbf{v}) - \frac{1}{2\theta_k}(\mathbf{C}^{(k)} \cdot \mathbf{C}^{(k)} - \mathbf{I}^{(k)}) \tag{25}$$

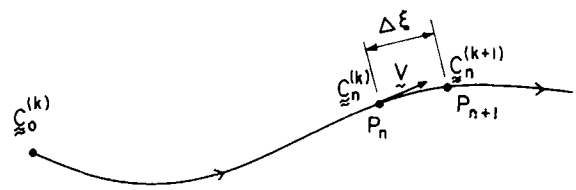

Figure 6. Sketch showing integration of elastic deformation tensor $\mathbf{C}^{(k)}$ along a streamline

where ξ is the distance along streamline (Figure 6). Usually the value of $\mathbf{C}_o^{(k)}$ at the upstream boundary is assigned, and marching forward in steps $\Delta\xi \ll \theta_k |\mathbf{v}|$ is satisfactory. For the higher modes the relaxation times rapidly decrease, and local equilibrium often may be assumed. In such cases, equation (22) may be used. The interation for $\mathbf{v}$ and p is then turned into an evolutionary process by replacing equation (16) with

$$\rho \frac{\partial v}{\partial t} = -Vp + \nabla \cdot \boldsymbol{\tau}' \tag{26}$$

In iteration Upadhyay took the 'old' values to evaluate $\nabla \cdot \boldsymbol{\tau}'$ in equation (26) and to replace $\partial \mathbf{v}/\partial t$ as a linear expression for $\mathbf{v}$ using backward difference and time step Δt. Equations (17) and (26) were then solved in a conventional FEM with variables $\mathbf{v}$ and p. After each step Δt, $\mathbf{C}^{(k)}$ was recalculated from equation (25), hence $\boldsymbol{\tau}'$ from equation (20), and the cycle repeated until convergence. Gaussian quadrature was employed to evaluate area integrals involving $\mathbf{C}^{(k)}$ over each element, which occur because of the Galerkin procedure in the FEM.

Example and comparison with experiment

The above scheme has been applied to the channel shown in Figure 5(a), with $h_1 = 0{\cdot}795$ cm, $h_2 = 0{\cdot}108$ cm, $\alpha = 14{\cdot}3°$, and width 20 cm. Experimentally the stresses were measured by A. I. Isayev at Cornell through the birefringence technique. The fluid was a sample of polyisobutylene Vistanex Lm.MH (Enjay). Figure 7 whows the rheometric data (in

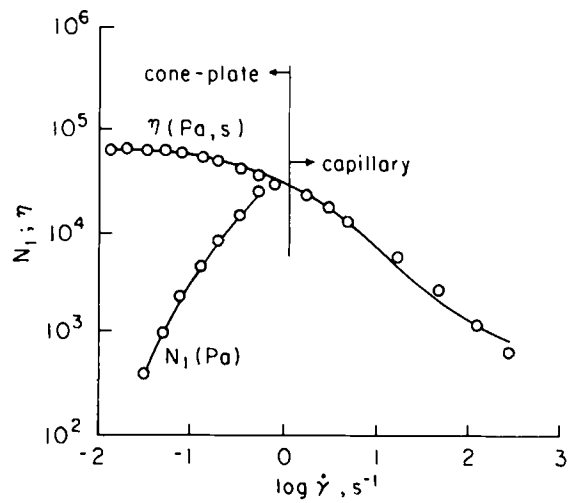

Figure 7. Rheological characterization curves of test material: η (apparent viscosity) and N_1 (first normal stress difference) versus shear rate $\dot{\gamma}$. Symbols: experimental points; curves: two mode Leonov model with fitted parameters

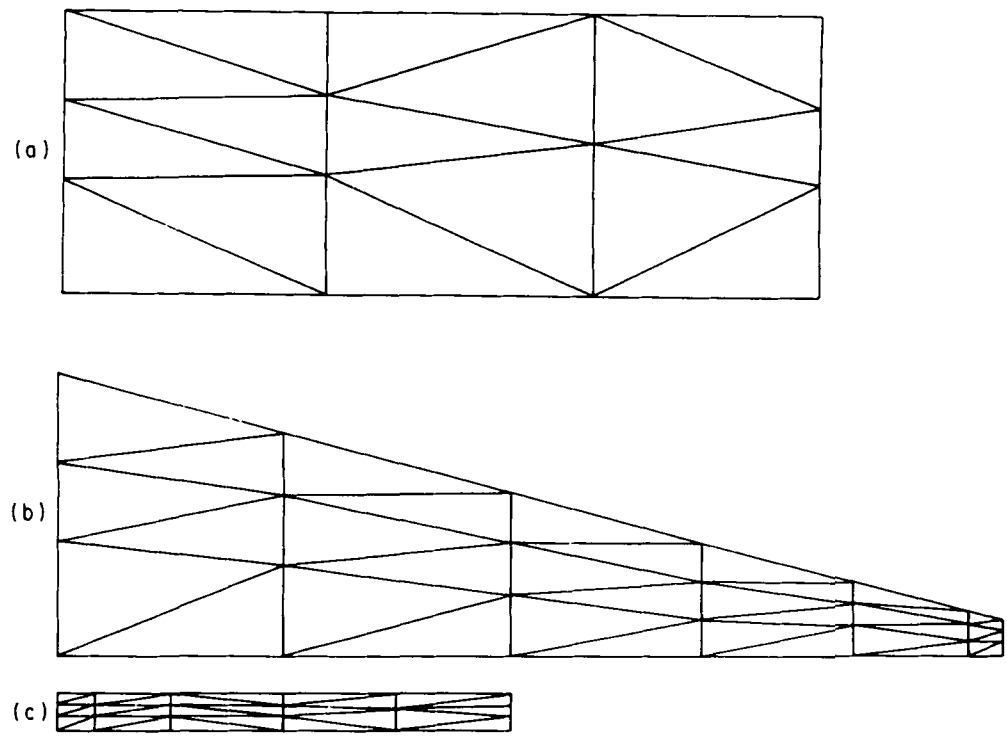

Figure 8. Finite-element mesh of 439 unknowns, used for the test problem of type (a) of Figure 5; (a) the wide section ($h_1 = 0{\cdot}795$ cm); (b) the tapered section ($\alpha = 14{\cdot}3°$); (c) the narrow section ($h_2 = 0{\cdot}108$ cm)

circles) of the shear viscosity η and the first normal stress difference N_1, as functions of the shear rate $\dot{\gamma}$. The solid curve is a two-mode Leonov-model fit with the following parameters: $s = 0{\cdot}01$, $\eta_1 = 3{\cdot}58 \times 10^4$ Pa.s., $\theta_1 = 6{\cdot}07$ s, $\eta_2 = 2{\cdot}95 \times 10^4$ Pa.s, $\theta_2 = 0{\cdot}47$ s.

At both up- and downstream ends, the fully developed velocity profiles, far from being parabolic, can be readily solved. These are listed in Reference 11. The solution provides the initial data $\mathbf{C}_0^{(k)}$ along the upstream boundary. Computations are then carried out for four different flow rates Q, ranging from $0{\cdot}1456 \times 10^{-7}$ m^3/s to $2{\cdot}387 \times 10^{-7}$ m^3/s. Based upon θ_1 and the average shear rate in the smaller channel (the average velocity divided by the half gap), the Deborah number ranges from 7·6 to 124. The FEM mesh using triangular elements is shown in Figure 8, with linear interpolation for p and quadratic for u, v in the usual manner. The C_{ij}s are defined at the corner and midside nodes such as u and v. In the example, 439 unknowns are used, and the computation ran smoothly for all cases studied. The resulting stresses are converted into birefringence Δn according to the stress optical law: $\Delta n = C\sqrt{(N_1^2 + 4\tau_{12}^2)}$, where $C = 1{\cdot}414 \times 10^{-9}$ Pa^{-1} is the stress optical coefficient (separately determined by experiment). A typical comparison is given in Figure 9, showing the birefringence variation along the centreline. The agreement is excellent except at the highest flow rate, hence highest Deborah number. Based on our experience in other applications,[9] a 3-mode Leonov model should lead to better prediction in the latter case. For details and more results see Reference 11.

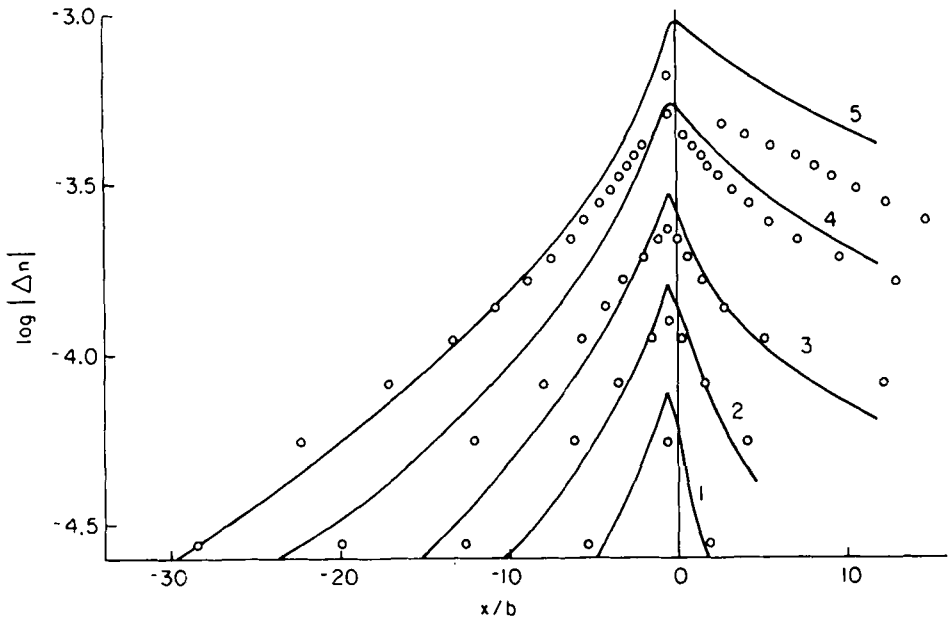

Figure 9. Birefringence Δn along centreline for flow going from the wide channel to the narrow. Numbers 1, 2, 3, 4 referring to increasing flow rates; circles: experimental data. More details in Reference 10

CONCLUDING REMARKS

We have presented only an outline of FEM simulation of two key problems of flow simulation of injection moulding processes, as recently developed at Cornell. The fluid is highly non-Newtonian and temperature sensitive, and the difficulty is compounded by moving boundaries, interaction with transient heat transfer, and visco-elasticity. To report the detailed treatments is beyond the scope of this paper. The numerical examples, though of relatively simple geometry, appear to establish the soundness of the programs. Further improvement on accuracy and efficiency, as well as applications to practical problems, seem worthwhile.

In the cavity filling problem, the advantage of the boundary-integral method in reducing the spatial dimensions by one makes it a potentially attractive approach to tackle complicated cavity configurations, e.g. of irregular shape with inserts. Although internal elements must still be used, they do not control the accuracy of the solution as much as in the conventional FEM. It may serve more readily as the basis of more approximate treatments trading off accuracy against computing cost.

The FEM program incorporating the Leonov viscoelastic model to solve the sample juncture problem has encountered no difficulty at *De* exceeding 100. The Deborah number here has been defined in terms of the longest relaxation time, and is, like the Reynolds number, obviously of only qualitative significance. As an indicator for the relative importance of the elastic effects of viscous effects, at large deformation rates and in a complex flow it should be based on an *effective* relaxation time. This unfortunately causes ambiguity when multi-modes are used in the constitutive model. We believe the Leonov model should be adequate for high elasticity state, and the integration procedure has faithfully followed the zone of influence. Although no mesh refinement study was made to ascertain the accuracy,

comparison with experimental data was satisfactory. It holds great promise for realistic predictions of such features as the juncture pressure loss, maximum stresses and orientation important to industrial applications.

ACKNOWLEDGEMENT

This work as well as the research at Cornell quoted were supported by NSF Grant 78-18868.

REFERENCES

1. C. A. Hieber and S. F. Shen, 'A Finite-element/finite-difference simulation of the injection-molding filling process', *J. Non-Newtonian Fluid Mech.*, **7,** 1–32 (1980).
2. T. H. Kwon, 'Application of the boundary integral method to the non-isothermal flow of a polymeric fluid advancing in a thin cavity of arbitrary shape', *M.S. Thesis*, Cornell University, 1982.
3. M. A. Morjaria, 'Finite-element methods for Newtonian and non-Newtonian fluids in creeping flow', *M.S. Thesis*, Cornell University, 1978.
4. M. Viryayuthakorn and B. Caswell, 'Finite-element simulation of viscoelastic flow', *J. Non-Newtonian Fluid Mech.*, **6,** 245–267 (1980).
5. M. J. Crochet and R. Kennings, 'Die swell of a Maxwell fluid: numerical predictions', *J. Non-Newtonian Fluid Mech.*, **7,** 199–212 (1980).
6. A. I. Leonov, 'Non-equilibrium thermodynamics and rheology of viscoelastic polymer midia', *Rheologica Acta*, **15,** 85–98 (1976).
7. P. A. Dashner and W. F. Van Arsdale, 'A phenomenological theory for elastic fluids', *J. Non-Newtonian Fluid Mech.*, **8,** 59–67 (1981).
8. A. I. Isayev, C. A. Hieber, R. K. Upadhyay and S. F. Shen, 'Time-dependent rheological behavior of polymer systems', in G. Astarita, G. Marracci and L. Nicolais (eds), *Rheology*, Vol. 3, Plenum, New York, 1980, pp. 91–98.
9. R. K. Ipadhyay, A. I. Isayev and S. F. Shen, 'Transient shear flow behavior of polymeric fluids according to the Leonov model', paper presented at *53rd Annual Meeting, the Society of Rhology*, Louisville, KY, October 1981.
10. A. I. Isayev and C. A. Hieber, 'Oscillatory shear flow of polymeric systems', *J. Polym. Sci., Phys. Ed.*, **20,** 423–440 (1982).
11. R. K. Upadhyay: 'Viscoelastic flow problems in injection molding and their simulation', *Ph.D. Thesis*, Cornell University, 1982.
12. G. Williams and H. A. Lord, 'Molding filling studies for the injection molding of thermoplastic materials', Parts I and II, *Polymer Eng. Sci.*, **15,** 553 (1975).
13. M. A. Jawson and G. T. Symm, *Integral Equation Methods in Potential Theory and Elastostatics*, Academic Press, 1977.
14. C. A. Brebbia, *The Boundary Element Method for Engineers*, Wiley, New York, 1978.
15. K. Y. Wang, 'An analysis of the frozen layer behind an advancing viscous fluid in a cold channel', *M.S. Thesis*, Cornell University, 1982.
16. R. B. Bird, R. C. Armstrong and O. Hassager, *Dynamics of Polymeric Liquids, Vol. 1*, Wiley, New York, 1977.